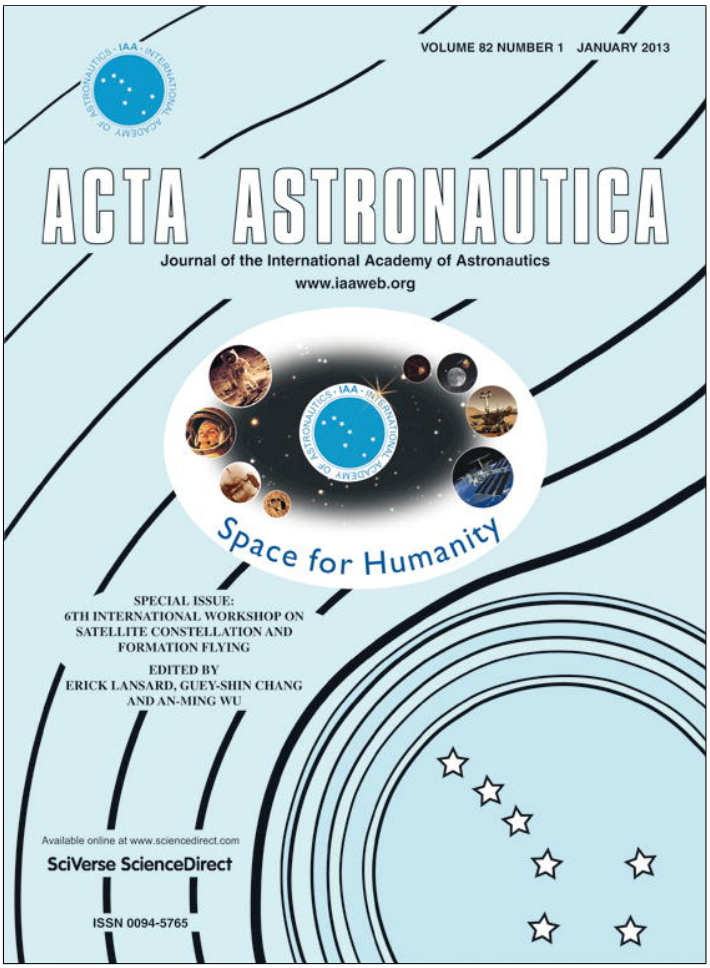

Acta Astronautica 82 (2013) 60–68

Contents lists available at SciVerse ScienceDirect

Acta Astronautica

journal homepage: www.elsevier.com/locate/actaastro

The design of observers for formation-flying control

Sašo Blažič [a,b], Drago Matko [a,b,*], Tomaž Rodič [a,c], Dejan Dovžan [b], Gašper Mušič [a,b], Gregor Klančar [a,b]

[a] SPACE-SI, Aškerčeva cesta 12, Ljubljana, Slovenia
[b] University of Ljubljana, Faculty of Electrical Engineering, Ljubljana, Slovenia
[c] University of Ljubljana, Faculty of Natural Sciences, Ljubljana, Slovenia

ARTICLE INFO

Article history:
Received 1 December 2011
Received in revised form
2 April 2012
Accepted 17 April 2012
Available online 15 May 2012

Keywords:
Formation flying
Image-based control
Observers

ABSTRACT

In this paper a method for estimating the relative orbit is proposed. The method requires a minimum number of simple sensors. The design of observers for formation-flying control, which is formulated as a control problem of tracking the target satellite, is treated. If the equations of the relative motion of the target and the chaser satellites are rewritten in the Local Vertical/Local Horizontal (LVLH) coordinate system, a nonlinear control system of the sixth order is obtained. It is very well known that such a control problem can be solved by a (linear or nonlinear) state controller. The formation-flying models are reviewed and analysed with respect to their observability according to the measured quantities. Based on the results of the observability analysis two state observers enabling an estimation of all the states are proposed in the paper: a simple observer of the linearised system and a nonlinear observer. Since cheap, small satellites are targeted, the application of cheap sensors is studied. In addition, the possibility of measuring the three relative position coordinates of the chaser satellite with a camera and a compass is given with some simulation results demonstrating the suppression of the measurement noise, which is significant when using cheap, COTS sensors and cameras.

1. Introduction

In Slovenia a new Slovenian Centre of Excellence for Space Sciences and Technologies Space-SI was established at the end of 2009, with the main focus on nano- and micro-satellite technologies. The Research & Technical Development (RTD) goals of the Space-SI consortium, consisting of academic institutions, high-tech small and medium enterprises and large industrial and insurance companies, are focused on nano- and micro-satellite technologies that enable high-precision interactive remote sensing and the precise manoeuvreing of small spacecrafts in formation-flying missions.

Nano-satellites, such as the Cubesat family, for example, are a very popular and affordable means of training young scientists and engineers at universities that have ambitious multidisciplinary goals in space RTD. The introduction of Commercial off-the-shelf (COTS) components has reduced the costs of small satellites considerably. This allows the introduction of new, creative paradigms that allow high-risk, high-benefit approaches in space-system design and mission planning, which are expected to accelerate technology development in unprecedented ways. These indicated transitions have opened up opportunities for newcomers to the space arena, including RTD players from economically less powerful and aerospace-developed regions. In a similar way, one could define RTD challenges for other types of missions

* Corresponding author at: SPACE-SI, Aškerčeva cesta 12, Ljubljana, Slovenia.
E-mail address: drago.matko@fe.uni-lj.si (D. Matko).

0094-5765/$ - see front matter © 2012 Elsevier Ltd. All rights reserved.
http://dx.doi.org/10.1016/j.actaastro.2012.04.035

that offer great science and technology opportunities for the small-satellite sector. This opens up very large RTD areas where we have identified the most promising RTD targets with an additional added value, which will be achieved by harmonising the individual RTD strategies of laboratories by focussing on a common, multidisciplinary goal targeted on enabling technologies for advanced platform manoeuvring.

In recent years there has been an increased interest in formation-flying satellites and autonomous docking. These formation-flying satellites offer potentially greater scientific and operational capabilities than those attainable with a monolithic spacecraft. Not only are the modules from a large and expensive monolithic satellite distributed to a number of smaller and cheaper satellites, but even more importantly a whole spectrum of new missions (such as stereo vision) that could be performed by a group of satellites is made possible.

The fundamentals of astrodynamics and a comprehensive treatment of the dynamics of space systems, including formation flying, are treated in standard textbooks [1,2]. The simplified dynamics of earth-orbiting formations represented by linear models of formations is based on the Hill–Clohessy–Wiltshire (HCW) [3,4]. Understanding and utilising the dynamics of relative motion is important for satellite-formation control [5,6]. The relative positions of the satellites in a formation can be estimated in several ways. A precise, but demanding, method is the global positioning system (GPS) [7–9], while vision-based navigation [10,11] represents a modern and promising method that can be used for measuring the relative line-of-sight vector [12]. In the case of simple sensors the observability of a system plays a crucial role in the orbit determination [13].

In this paper a method for estimating the relative orbit is proposed; this method requires a minimum number of simple sensors. The paper is organised as follows: In Section 2 the formation-flying models are reviewed and analysed with respect to their observability according to the measured quantities. Based on the results of the observability analysis a state observer based on simple sensors and enabling an estimation of all the states is proposed in Section 3. The role of observers in orbits' manoeuvering is illustrated by a simulation in Section 4.

2. Models of formation flying

The most common ways to describe formation flying are the general nonlinear equations of relative motion without disturbing accelerations [6,14,15,3,4]:

$$\ddot{x}-2\dot{\varphi}_R\dot{y}-\ddot{\varphi}_R y-\dot{\varphi}_R^2 x=-\frac{\mu(R+x)}{((R+x)^2+y^2+z^2)^{3/2}}+\frac{\mu}{R^2} \tag{1}$$

$$\ddot{y}+2\dot{\varphi}_R\dot{x}+\ddot{\varphi}_R x-\dot{\varphi}_R^2 y=-\frac{\mu y}{((R+x)^2+y^2+z^2)^{3/2}} \tag{2}$$

$$\ddot{z}=-\frac{\mu z}{((R+x)^2+y^2+z^2)^{3/2}} \tag{3}$$

where $\ddot{\varphi}_R$ is the angular acceleration of the target satellite; μ is the Earth's gravitational constant; $\dot{\varphi}_R$ is the angular velocity of the target satellite (in the case of a circular orbit it is the same as the mean motion); R is the radial distance of the target satellite; and x, y and z are the coordinates of the chaser satellite in the local vertical/local horizontal (LVLH) coordinate system of the target satellite. The coordinate system is centred in the target's center of mass. The y-axis of the LVLH coordinate system lies in the orbital plane and points in the direction of the flight; the x-axis points in the direction of the radius; while the z-axis completes the right-handed coordinate system. The movement of the target satellite is described by

$$\ddot{R}=R\dot{\varphi}_R^2-\frac{\mu}{R^2} \tag{4}$$

$$\ddot{\varphi}_R=-\frac{2\dot{R}\dot{\varphi}_R}{R} \tag{5}$$

These equations include the influence of the eccentricity and nonlinear differential gravitations. For close formation flying and small eccentricities these equations can be linearised [6]. If the target satellite has a circular orbit, its angular acceleration is zero ($\ddot{\varphi}_R=0$), and then $\dot{\varphi}_R$ becomes the mean motion

$$\dot{\varphi}_R=n=\sqrt{\frac{\mu}{R^3}} \tag{6}$$

So a linearised model of the movement of the chaser satellite with respect to the target satellite is obtained. The accelerations a_x, a_y, a_z in the x, y and z directions, respectively, can be included into equations to control the position and velocity of the chaser satellite. So the following Hill–Clohessy–Wiltshire (HCW) equations with disturbing accelerations are obtained:

$$\ddot{x}-2n\dot{y}-3n^2x=a_x$$

$$\ddot{y}+2n\dot{x}=a_y$$

$$\ddot{z}+n^2z=a_z \tag{7}$$

If we transform these equations to the state space, the state transition and input matrices are

$$\dot{\boldsymbol{\xi}}=\mathbf{A}\boldsymbol{\xi}+\mathbf{B}\mathbf{u}$$

$$\boldsymbol{\chi}=\mathbf{C}\boldsymbol{\xi} \tag{8}$$

where the state vector consists of the position and the velocity: $\boldsymbol{\xi}=[x\ y\ z\ \dot{x}\ \dot{y}\ \dot{z}]^T$, the control vector is $\mathbf{u}=[a_x\ a_y\ a_z]$, the vector of measured outputs is $\boldsymbol{\chi}$, and the corresponding matrices are

$$\mathbf{A}=\begin{bmatrix}0&0&0&1&0&0\\0&0&0&0&1&0\\0&0&0&0&0&1\\3n^2&0&0&0&2n&0\\0&0&0&-2n&0&0\\0&0&-n^2&0&0&0\end{bmatrix}\quad \mathbf{B}=\begin{bmatrix}0&0&0\\0&0&0\\0&0&0\\1&0&0\\0&1&0\\0&0&1\end{bmatrix}$$

The output matrix $\mathbf{C}$ depends on measurable quantities and is given in Table 1. The system is observable if the entire state $\boldsymbol{\xi}$ can be determined with measurable quantities, i.e., if the observability matrix

Table 1
The output **C** matrix and the overview of the observability.

Vector χ^T	Matrix **C**	Rank **Q**	Vector χ^T	Matrix **C**	Rank **Q**
$[x,y,z]$	$\begin{bmatrix}1&0&0&0&0&0\\0&1&0&0&0&0\\0&0&1&0&0&0\end{bmatrix}$	6	$[x,y,\dot{z}]$	$\begin{bmatrix}1&0&0&0&0&0\\0&1&0&0&0&0\\0&0&0&0&0&1\end{bmatrix}$	6
$[\dot{x},y,z]$	$\begin{bmatrix}0&0&0&1&0&0\\0&1&0&0&0&0\\0&0&1&0&0&0\end{bmatrix}$	6	$[\dot{x},\dot{y},z]$	$\begin{bmatrix}0&0&0&1&0&0\\0&0&0&0&1&0\\0&0&1&0&0&0\end{bmatrix}$	5
$[\dot{x},\dot{y},\dot{z}]$	$\begin{bmatrix}0&0&0&1&0&0\\0&0&0&0&1&0\\0&0&0&0&0&1\end{bmatrix}$	5	$[x,y]$	$\begin{bmatrix}1&0&0&0&0&0\\0&1&0&0&0&0\end{bmatrix}$	4
$[x,z]$	$\begin{bmatrix}1&0&0&0&0&0\\0&0&1&0&0&0\end{bmatrix}$	5	$[y,z]$	$\begin{bmatrix}0&1&0&0&0&0\\0&0&1&0&0&0\end{bmatrix}$	6
$[x,\dot{z}]$	$\begin{bmatrix}1&0&0&0&0&0\\0&0&0&0&0&1\end{bmatrix}$	5	$[y,\dot{z}]$	$\begin{bmatrix}0&1&0&0&0&0\\0&0&0&0&0&1\end{bmatrix}$	6
$[\dot{x},z]$	$\begin{bmatrix}0&0&0&1&0&0\\0&0&0&0&0&1\end{bmatrix}$	4	$[\dot{y},z]$	$\begin{bmatrix}0&0&0&0&1&0\\0&0&0&0&0&1\end{bmatrix}$	5
$[x]$	$[1\ 0\ 0\ 0\ 0\ 0]$	3	$[y]$	$[0\ 1\ 0\ 0\ 0\ 0]$	4
$[z]$	$[0\ 0\ 1\ 0\ 0\ 0]$	2	$[\dot{y}]$	$[0\ 0\ 0\ 0\ 1\ 0]$	3

$$\mathbf{Q}=\begin{bmatrix}\mathbf{C}\\ \mathbf{CA}\\ \mathbf{CA}^2\\ \vdots\\ \mathbf{CA}^{n-1}\end{bmatrix} \tag{9}$$

has a full rank n, in our case $n=6$ [16].

By observing Table 1 it becomes clear that the system is observable if at least the position y and either position z or its time derivative $\dot{z}$ are measurable.

The system state can be estimated by state observers. A state observer is a system that models a real system in order to provide an estimate of its internal state, given measurements of the input and the output of the real system, and is described as follows:

$$\dot{\hat{\boldsymbol{\xi}}}=\mathbf{A}\hat{\boldsymbol{\xi}}+\mathbf{Bu}+\mathbf{H}(\boldsymbol{\chi}-\hat{\boldsymbol{\chi}})$$

$$\hat{\boldsymbol{\chi}}=\mathbf{C}\hat{\boldsymbol{\xi}} \tag{10}$$

where $\hat{\boldsymbol{\xi}}$ is the estimated state vector and **H** is the observer matrix designed using an appropriate method (e.g., pole placement). From linear equations (7) it can be seen that the linear model is decoupled into two subsystems: the movement in the $x-y$ plane and the movement in the z direction. The z subsystem is observable if either z or $\dot{z}$ are measurable. The $x-y$ subsystem is observable if and only if y is measurable. If additional quantities are measured, the observers can be used to improve the estimation and are usually referred to as Kalman filters.

The nonlinear observer is based on the nonlinear model

$$\dot{\boldsymbol{\xi}}=\mathbf{f}(\boldsymbol{\xi},\mathbf{u},\dot{\varphi}_R,\ddot{\varphi}_R,R)$$

$$=\begin{bmatrix}\xi_4\\ \xi_5\\ \xi_6\\ 2\dot{\varphi}_R\xi_5+\ddot{\varphi}_R\xi_2+\dot{\varphi}_R^2\xi_1-\frac{\mu(R+\xi_1)}{((R+\xi_1)^2+\xi_2^2+\xi_3^2)^{3/2}}+\frac{\mu}{R^2}\\ -2\dot{\varphi}_R\xi_4-\ddot{\varphi}_R\xi_1+\dot{\varphi}_R^2\xi_2-\frac{\mu\xi_2}{((R+\xi_1)^2+\xi_2^2+\xi_3^2)^{3/2}}\\ -\frac{\mu\xi_3}{((R+\xi_1)^2+\xi_2^2+\xi_3^2)^{3/2}}\end{bmatrix}$$

$$\boldsymbol{\chi}=\mathbf{C}\boldsymbol{\xi} \tag{11}$$

and can be written as follows:

$$\dot{\hat{\boldsymbol{\xi}}}=\mathbf{f}(\hat{\boldsymbol{\xi}},\mathbf{u},\dot{\varphi}_R,\ddot{\varphi}_R,R)+\mathbf{H}(\boldsymbol{\chi}-\hat{\boldsymbol{\chi}})$$

$$=\begin{bmatrix}\hat{\xi}_4\\ \hat{\xi}_5\\ \hat{\xi}_6\\ 2\dot{\varphi}_R\hat{\xi}_5+\ddot{\varphi}_R\hat{\xi}_2+\dot{\varphi}_R^2\hat{\xi}_1-\frac{\mu(R+\hat{\xi}_1)}{((R+\hat{\xi}_1)^2+\hat{\xi}_2^2+\hat{\xi}_3^2)^{3/2}}+\frac{\mu}{R^2}\\ -2\dot{\varphi}_R\hat{\xi}_4-\ddot{\varphi}_R\hat{\xi}_1+\dot{\varphi}_R^2\hat{\xi}_2-\frac{\mu\hat{\xi}_2}{((R+\hat{\xi}_1)^2+\hat{\xi}_2^2+\hat{\xi}_3^2)^{3/2}}\\ -\frac{\mu\hat{\xi}_3}{((R+\hat{\xi}_1)^2+\hat{\xi}_2^2+\hat{\xi}_3^2)^{3/2}}\end{bmatrix}$$
$$+H(\boldsymbol{\chi}-\hat{\boldsymbol{\chi}})$$

$$\hat{\boldsymbol{\chi}}=\mathbf{C}\hat{\boldsymbol{\xi}} \tag{12}$$

where ξ_i and $\hat{\xi}_i$ stand for the i-th component of the vectors $\boldsymbol{\xi}$ and $\hat{\boldsymbol{\xi}}$, respectively.

3. Measurement based on simple sensors

We have already established that by measuring y and z in the LVLH coordinate system of the target satellite we can

design an observer that is able to recover the full state. If we add the measurement of x, the quality of the state estimation generally improves. A direct measurement of $\dot{x}$, $\dot{y}$ and $\dot{z}$ is very difficult, so we will rely in our approach on a measurement of the position only. The key question is: what measurements are available when using simple sensors if the goal is to have a full state estimation? Without having any information about the target orbit and without having any relative measurement, such as differential GPS (e.g., if the target is not cooperative), it is very hard to reconstruct all the states. We assume here that the chaser is equipped with a camera and a sensor that can measure the distance between the two objects. Any possible measurements are only available in the chaser coordinate system. The transformation to the target coordinates will be discussed later.

3.1. The proposed concept

Let us first focus on the measurement of the x coordinate in the LVLH system of the chaser (x-axis lies along the radius vector, positive away from the center of the Earth). Since the LVLH coordinates are used for the near-circular orbits (although the approach can be extended to elliptic orbits), the problem of determining x reduces to (Fig. 1, left)

$$x = d \sin \alpha \tag{13}$$

where d is the distance between the target and the chaser, and α is the angle between the line that connects both objects and the y–z plane (the plane tangential to the orbit at the position of the chaser). It should be noted that the tangent in Fig. 1 (left part) does not, in general, coincide with the y-axis. The angle between this tangent and the horizon β can be calculated as follows:

$$\beta = \arccos \frac{R_E}{R_E + h} \tag{14}$$

where R_E is the radius of the Earth and $h = R - R_E$ is the height of the satellite above the Earth's surface. The idea of the suggested approach is to estimate the angle $\gamma = \alpha + \beta$, i.e., the angle between the target and the horizon if observed from the position of the chaser. The coordinate x is then calculated using

$$x = d \sin \alpha = d \sin(\gamma - \beta) \tag{15}$$

where β is obtained from the geometry of the orbit, γ from the visual based measurement, and the inter-satellite distance d is measured.

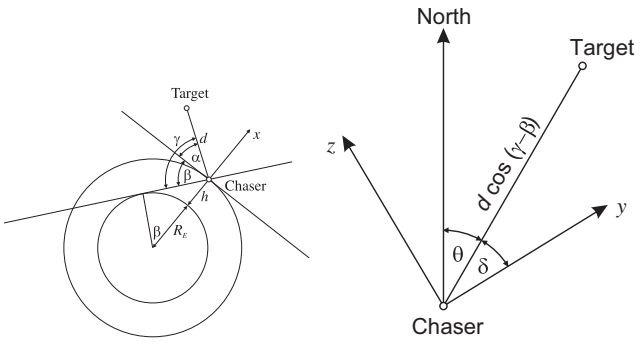

Fig. 1. The geometry of the x (left) and z (right) estimation.

Although it is not necessary to have the target stabilised in the centre of the image, this is very useful since it can help when estimating x if the horizon is lost from the image. Normally, the target would be brought into the image centre by applying some simple, visual-based, orientation control. The measurement of γ becomes difficult if the horizon is not visible in the image. This is why wide-angle (or omni-directional) cameras are preferable. If the image is stabilised, then the information about the angle γ can be obtained by taking into account the measurement from the gyros, but this approach results in a poor (drifted) estimation, because it requires the integration of signals with a relatively high level of noise.

The coordinate z in the chaser frame is defined as the distance between the orbital plane of the chaser and the target (Fig. 1, right). It can be deduced by stabilising the target in the centre of the chaser's camera image. By using a compass the angle of the satellite's orientation (it is oriented towards the other satellite) in the (y, z) plane relative to the north can be obtained (this measurement is very inaccurate when the satellite is in the polar region)—this angle is denoted by θ in Fig. 1 (right). The orientation of the tangential direction relative to the north (denoted by $\theta + \delta$ in Fig. 1) in each point is known in advance since the orbit is known very accurately. By subtracting these two angles the δ angle is obtained, which is used for the determination of z and y

$$z = d \cos \alpha \sin \delta \tag{16}$$

$$y = d \cos \alpha \cos \delta \tag{17}$$

We have already said that for the purpose of control the system has to be described in the LVLH frame of the target, while all the measurements discussed above are taken in the LVLH frame of the chaser. We only treat the case of a low Δv-budget (a few, up to a few tens of, metres per second), and consequently the close formation flying is only possible if the two orbits are very close together, which results in the chaser and the target LVLH frames lying almost in parallel. Let us try to substantiate this statement. Both frames have a different orientation if the satellites fly apart or one of them uses propulsion. If the whole $\Delta v = 20$ m/s budget were theoretically used in a single thrust in the cross-track direction, the vector of velocity would rotate by less than 10 arc min. Since in the proposed case the satellites fly in close formation – up to 1 km apart – the velocity vector in the same orbit is up to a half of an arc minute different. To sum up, in our case both frames do lie almost in parallel (the difference is at most in the arc-minutes range) and the transformation from one system to another only consists of changing the sign of the obtained measurements.

3.2. Choice of sensor

Satellite formation flying requires a relative satellites' pose estimation. Different sensors have been applied to tackle this problem [17]. Probably the best choice is the use of CDGPS (carrier differential global positioning system) where a 1-cm 3D position accuracy can be achieved [18]. This approach requires some computational power,

communication bandwidth and can only be used in a cooperating, predefined, group of satellites. The range is limited by the communication reach. A similar idea using radio spread-spectrum ranging can also be applied at greater distances where the expected accuracy is 10 cm [19,20].

Another promising method includes a laser rangefinder, which is a very good sensor for determining the relative pose estimation, with a 1-mm distance and a 0.5° angle accuracy being easily obtained [21]. The use of lasers requires constant target tracking, which can be problematic if the relative distance and attitude are changing quickly. The approach, however, does not require a cooperating target. A real application of the presented approach should apply the combination of a camera and a laser-ranging approach. The camera is used for tracking the target satellite and obtaining the course estimation of the relative position, while the laser ranging gives an accurate relative pose estimate.

The approaches mentioned above are relatively expensive and we only plan to use a camera and a magnetometer as sensors of the relative position of the satellites. We assume that during the satellite's operation the roll movement is stabilised (in such a case the horizon would be made horizontal on the image). As mentioned before, we also have to implement some visual-based control algorithm [22] to keep the other satellite in the centre of the camera image. Then we have to estimate the angle between the satellite and the horizon (denoted by γ in Fig. 1), the distance to the satellite (d) and the azimuth of the target satellite with respect to the chaser (denoted by θ in Fig. 1). The angular accuracy depends on the camera's horizontal and vertical resolution and its field of view (FOV). Supposing a HFOW (horizontal field of view) of 50° and a horizontal resolution of 640 pixels, a one-pixel accuracy means 0.08° accuracy. In practice, the line of the horizon may not be very easy to determine (a few-pixel error is made), while the angle β can be obtained very accurately. However, we estimate that a precision of 0.5° for the angle α should be possible to obtain. The distance to the target can be estimated by recognising at least three known points on the target image or recognising the known target shape on the image. If chasing the cooperative satellite (which is our primary goal), the problem is simplified by marking the edges of the satellite with active markers, such as light-emitting diodes. By knowing the camera's parameters (focal length), the accuracy again depends on the camera's resolution and also on the lens distortion (fish eye). The camera error caused by the lens distortion can be rectified if the lens-distortion model is known. If the distance between the known points on the target satellite (which is similar to the size of the satellite) is D_t, then the angle between these points from the viewpoint of the chaser is $2\arctan D_t/2d$. This angle can easily be converted into pixels. If we are able to estimate this distance from the image with an error in the one-pixel range (this error does not depend on the distance), the relative error of the distance measurement grows approximately linearly with the distance (if $2d \gg D_t$). The main source of error when estimating δ is the measurement of θ. The measurement accuracy due to the magnetometer is typically in the few-degrees range. The reports in the literature [23,24] show that a one-to-five degrees accuracy can be achieved with proper filtering.

4. The role of observers in orbit manoeuvres

In orbit manoeuvres such as, e.g., docking, the observers can be used to filter the measured signals. With cheap sensors, such as cameras that have a low image resolution, the signals are very noisy and the noise is even amplified when using controllers that require signal derivatives. However, using observers the signal derivatives can be obtained without the derivation of noisy signals.

In order to verify the proposed procedure, a simulation study was performed for a two-satellites constellation with an orbit period of 5837 s. The nonlinear model of the satellite formation was simulated. The respective angles were calculated and the simulated angles α and δ were corrupted with a Gaussian noise using a standard deviation of 0.5° and 5°, respectively. In the model of the camera, as a distance sensor, the target size was chosen as $D_t = 0.5$ m, and the standard deviation of the inter-marker distance in the image was 1 pixel, which results in a relative measurement error of approximately 7% at the inter-satellite distance of 25 m. If the distance d is larger than 1 m, the absolute measurement error grows approximately quadratically with d.

Since the measurement errors are not Gaussian, the observer matrix $\mathbf{H}$ was determined by optimisation with genetic algorithms. We used the genetic algorithm optimisation in the Genetic Algorithm and Direct Search Toolbox. The parameters were left at the default values. The fitness function used was

$$J = \int_0^{5T} ((\xi-\hat{\xi})^T\mathbf{V}(\xi-\hat{\xi}) + (\boldsymbol{\chi}-\hat{\boldsymbol{\chi}})^T\mathbf{N}(\boldsymbol{\chi}-\hat{\boldsymbol{\chi}}))\, dt. \tag{18}$$

where T is the period of the satellites. The matrix $\mathbf{V}$ was diagonal with the first three elements set to 1 and the remaining three set to 0.001. The matrix $\mathbf{N}$ represents the trade-off between the measurement and the state noise (it was chosen as a unity matrix multiplied by 100). The vectors ξ and $\boldsymbol{\chi}$ are the vector of the true states and the measured (corrupted) outputs from the nonlinear model, while $\hat{\xi}$ and $\hat{\boldsymbol{\chi}}$ come from the observer of the HCW model given by Eq. (10). Note that the nonlinear observer gives almost the same results because the satellites are kept close during our experiments. The resulting matrix $\mathbf{H}$ was

$$\mathbf{H}^T = 0.01\begin{bmatrix} 10.1030 & -0.00005 & 0 & 0.0103 & -0.0002 & 0 \\ -0.00005 & 3.3665 & 0 & 0.0002 & 0.0100 & 0 \\ 0 & 0 & 2.1357 & 0 & 0 & 0.0091 \end{bmatrix} \tag{19}$$

In a similar way, the controller gain $\mathbf{K}$ of the state controller ($\mathbf{u} = -\mathbf{K}\xi$) was obtained by optimising the fitness function

$$J = \int_0^{5T} (\xi^T\mathbf{Q}\xi + \mathbf{u}^T\mathbf{R}\mathbf{u})\, dt \tag{20}$$

with $\mathbf{Q}$ and $\mathbf{R}$, respectively, set to the same values as $\mathbf{V}$ and $\mathbf{N}$, respectively, above. The resulting controller gain

was

$$\mathbf{K} = 0.01\begin{bmatrix} 0.0992 & 0.3687 & 0 & 2.0472 & 1.7688 & 0 \\ 0.4719 & 2.1939 & 0 & 0.1253 & 5.7731 & 0 \\ 0 & 0 & 0.9069 & 0 & 0 & 80.5530 \end{bmatrix} \tag{21}$$

In the gain optimisation the control law was $\mathbf{u} = -\mathbf{K}\xi$, while in the closed-loop experiments the control law $\mathbf{u} = -\mathbf{K}\hat{\xi}$ was used.

Three experiments were conducted. The initial value of the state estimates is 0 in all cases. The first experiment was made in an open-loop operation with the initial condition of the system $\xi^T(0) = [0, 35, 35, 0.01556, 0, 0.000389]$, where the positions and the velocities are given in m and m/s, respectively. An elliptic relative orbit is chosen, where both satellites have the same orbit period (y does not drift), while the inter-satellite distance changes between 15 and 50 m. The relative positions are given in Fig. 2, where the measured (noisy), the estimated and the true coordinates of the satellite positions are shown. It is clear that the quality of the measurements relies heavily on the inter-satellite distance, while the quality of the estimates is well maintained throughout the experiment.

In the second experiment, the closed-loop operation was tested. The initial conditions were the same as before. The control goal was to drive the states to 0. No additional requirements were given, e.g., the transient without overshoot (this would be absolutely necessary for docking). The idea was just to show that the observed states can be used in a control application. Fig. 3 shows the measured (noisy), the estimated and the true coordinates of the satellite positions. Fig. 4 is only informative and shows the corresponding continuous control signals. In practice, however, the discrete pulses should be applied to the thrusters. Nevertheless, by analysing the control signals it can be seen that the Δv-budget of this manoeuvre is approximately 4 m/s, which is far too much for such a simple manoeuvre. In practice, such manoeuvres are done much more slowly and with a lower Δv-budget. The classical trade-off between the control effort and the control performance is not a topic of this work and the control performance will not be analysed further.

In the last experiment one satellite encircles the other at a constant inter-satellite distance (in our case the distance is 20 m). The experiment is done in the open-loop operation, i.e., the movements are the result of a natural motion. This trajectory is only possible if the plane of the circle is inclined by 60° relative to the orbit plane. Such an experiment is important where a constant inter-satellite distance is needed and the target should be seen from different viewpoints, e.g., for visual surveillance. The initial conditions of the system are $\xi^T(0) = [0, 20, 0, 0.01076, 0, 0.01865]$. The results are shown in Fig. 5.

5. Conclusion and future work

In this paper we have discussed the observability of the states of a formation with respect to the measurable quantities. Since cheap, small satellites are targeted, the application of cheap sensors (COTS technology) was studied. Two state observers are proposed in the paper: a simple observer of the linearised system (based on the HCW model) and a nonlinear observer. In addition, the possibility of measuring the three coordinates with a camera and a compass is given, with some simulation results demonstrating the suppression of the measurement noise. The simulations were done with realistic models of the sensors. The approach is simple and we

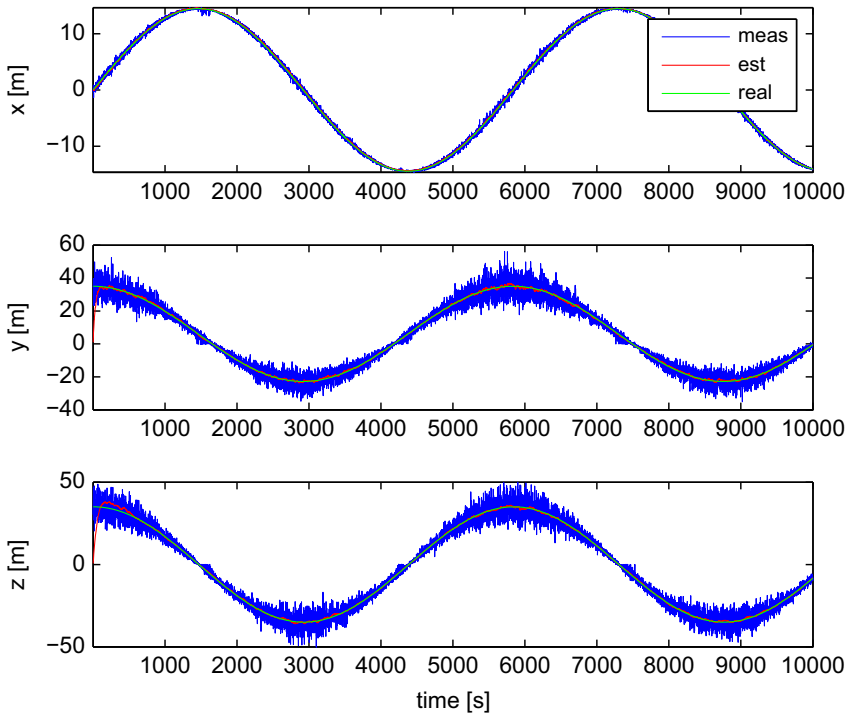

Fig. 2. The measured (noisy—blue), estimated (red) and true (green) coordinates of the chaser's position in the open loop. (For interpretation of the references to color in this figure caption, the reader is referred to the web version of this article.)

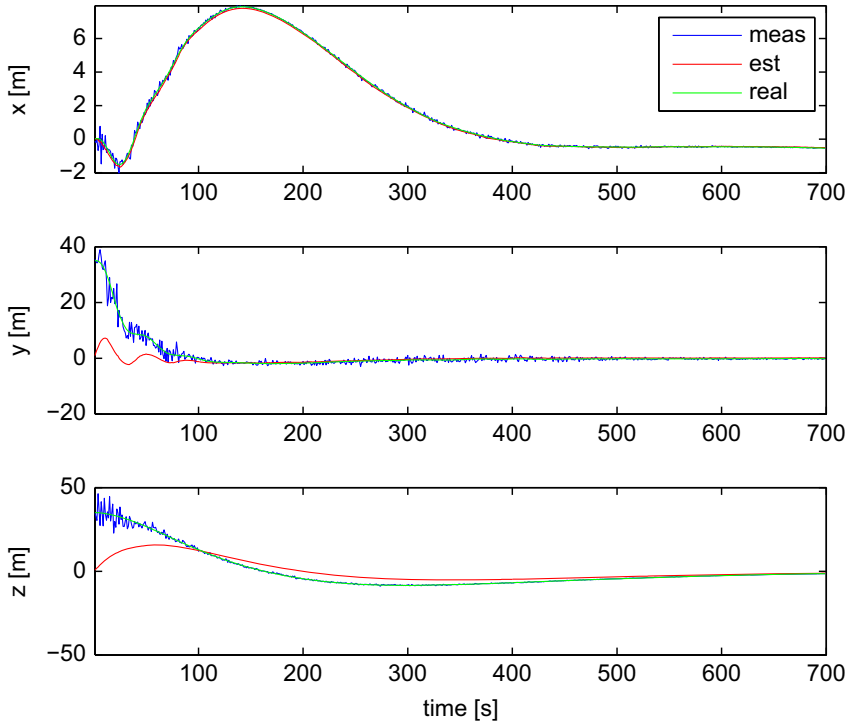

Fig. 3. The measured (noisy—blue), estimated (red) and true (green) coordinates of the chaser's position in the closed loop. (For interpretation of the references to color in this figure caption, the reader is referred to the web version of this article.)

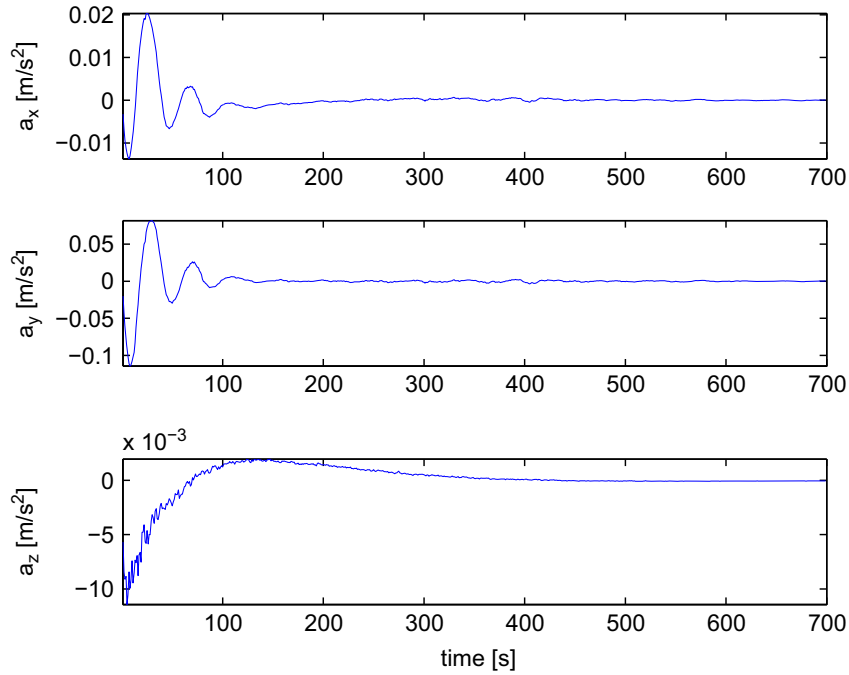

Fig. 4. The control signals.

believe that it is suitable for the implementation on nanosatellites. It is, however, limited for cases with low inter-satellite distance because it relies on optical sensors.

In its current structure, the Space-SI Centre of Excellence has the science and technology potential to streamline the prospective RTD niche areas of individual laboratories into a closed-loop solution for the development of enabling technologies for advanced spacecraft manoeuvring during formation flying as well as for high-precision remote sensing in Earth observation and photometry in astrophysics. Since all these important applications have a common requirement for precise micropropulsion and advanced control of micro/nanosatellite platforms, the Space-SI strategy is to integrate these areas into a multidisciplinary laboratory infrastructure for on-ground testing where investigations can be streamlined into closed-loop solutions ranging from micropropulsion with high-precision cold- and hot-gas

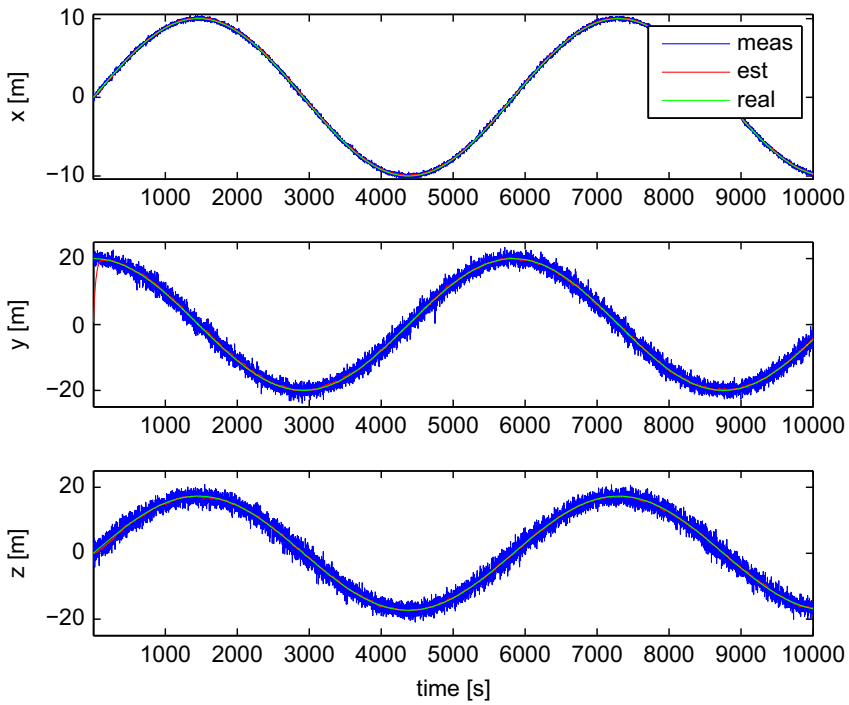

Fig. 5. The measured (noisy—blue), estimated (red) and true (green) coordinates of the chaser's position during the encircling experiment. (For interpretation of the references to color in this figure caption, the reader is referred to the web version of this article.)

micro-thrusters and vision-based control/servoing to applications in high-precision remote sensing and enabling the development of technologies for advanced spacecraft manoeuvring during formation flying.

Acknowledgement

The Centre of Excellence for Space Sciences and Technologies Space-SI is an operation part financed by the European Union, European Regional Development Fund and the Republic of Slovenia, Ministry of Higher Education, Science and Technology. The financial support of the Slovenian Research Agency for ARRS projects P2-219, L2-2378 and L2-0560 is also gratefully acknowledged.

References

[1] D.A. Vallado, Fundamentals of Astrodynamics and Applications, 2nd edition, Microcosm, Inc., 2001.
[2] H. Schaub, J.L. Jinkins, Analytical Mechanics of Space Systems, AIAA, Reston, VA, 2003, pp. 11–15, 593–673.
[3] S.R. Ploen, D.P. Scharf, F.Y. Hadaegh, A.B. Acikmese, Dynamics of earth orbiting formations, in: AIAA Guidance, Navigation and Control Conference, Providence, Rhode Island, 2004, available electronically from 〈http://hdl.handle.net/2014/38974〉.
[4] D.R. Izzo, Formation flying linear modelling, in: Proceedings of the 5th Conference on Dynamics of Systems and Structures in Space (DCSSS), Kings College, Cambridge, 2002.
[5] H.-H. Yeh, A. Sparks, Geometry and control of satellite formations, in: Proceedings of the American Control Conference Chicago, Illinois, 2000.
[6] V.V.S.S. Vaddi, Modelling and Control of Satellite Formations, Doctoral Dissertation, Texas A&M University, available electronically from 〈http://hdl.handle.net/1969.1/329〉, 2004.
[7] N.C. Nuzzo, Effects of Propagation Techniques on Relative GPS Navigation, Thesis (S.M.), Massachusetts Institute of Technology, 1999.
[8] J.-S. Ardaens, S. D'Amico, O. Montenbruck, Final commissioning of the PRISMA GPS navigation system, in: Proceedings of the 22nd International Symposium on Spaceflight Dynamics, Sao Jose dos Campos, Brazil, 2001.
[9] S. D'Amico, J.-S. Ardaens, R. Larsson, Spaceborne autonomous formation flying experiment on the PRISMA mission, in: Proceedings of the AIAA Guidance, Navigation, and Control Conference, Portland, USA, 2011 (accepted for publication in Journal of Guidance, Control, and Dynamics).
[10] R. Alonso, J.-Y. Du, D. Hughes, J.L. Junkins, J.L. Crassidis, Relative navigation for formation flying of spacecraft, in: Proceedings of the 2001 Flight Mechanics Symposium, Greenbelt, Maryland, NASA/CP–2001-209986, 2001.
[11] R. Alonso, J. Crassidis, J.L. Junkins, Vision-based relative navigation for formation flying of spacecraft, in: Proceedings of the 2000 AIAA, GNC Conference, Denver, CO, 2000, Paper 2000-4439.
[12] J.R. Yim, J.L. Crassidis, J.L. Junkins, Autonomous orbit navigation of two spacecraft system using relative line of sight vector measurements, in: Proceedings of the AAS Space Flight Mechanics Meeting, Maui, HI, 2004, Paper #04–257.
[13] J.R. Yim, J.L. Crassidis, J.L. Junkins, Autonomous orbit navigation of interplanetary spacecraft, in: AIAA/AAS Astrodynamics Specialist Conference, Denver, CO, 2000, pp. 53–61, AIAA Paper 2000-3936.
[14] S.S. Vaddi, S.R. Vadali, K.T. Alfriend, Formation flying: accommodating nonlinearity and eccentricity perturbations, J. Guidance Control Dyn. 26 (2) (2003) 214–223.
[15] U. Walter, Astronautics: The Physics of Space Flight, 2nd, Enlarged and Improved Edition, Wiley-VCH, Weinheim, Germany, 2012.
[16] K. Ogata, Modern Control Engineering, 5th edition, Prentice Hall, Boston, 2009.
[17] T. Rupp, S. D'Amico, O. Montenbruck, E. Gill, Autonomous formation flying at DLR's German space operations center (GSOC), in: 58th International Astronautical Congress, Hyderabad, India, 2007, Paper IAC-07-D1.2.01.
[18] S. Leung, O. Montenbruck, Real-time navigation of formation-flying spacecraft using global-positioning-system measurements, J. Guidance Control Dyn. 28 (2) (2005) 226–235.
[19] S. Wang, E. Zhang, Inter-satellite radio links and spread-spectrum ranging for satellite formation flying, in: 2002 3rd International Conference on Microwave and Millimeter Wave Technology (ICMMT) Proceedings, 2002, pp. 233–236.
[20] L. Chen, C. Zhang, B. Xu, Influence of sampling noise on spread-spectrum ranging based on software defined radio, in: The Tenth

International Conference on Electronic Measurement & Instruments ICEMI'2011, 2011, pp. 359–362.
[21] G. Peng, Y. Zheng, Characters of laser ranging on inter-satellite relative position measurement, in: 3rd International Conference on Recent Advances in Space Technologies RAST '07, 2007, pp. 614–617.
[22] G. Klančar, S. Blažič, D. Matko, G. Mušič, Image-based attitude control of a remote sensing satellite, J. Intell. Robotic Syst. 66 (3) 343–357.
[23] P. Appel, Attitude estimation from magnetometer and earth-albedo-corrected coarse sun sensor measurements, Acta Astronaut. 56 (1–2) (2005) 115–126.
[24] S.-W. Kim, M. Abdelrahman, S.-Y. Park, K.-H. Choi, Unscented Kalman filtering for spacecraft attitude and rate determination using magnetometer, J. Astron. Space Sci. 26 (1) (2009) 31–46.

Sašo Blažič received B.Sc., M.Sc., and Ph.D. degrees in 1996, 1999, and 2002, respectively, from the Faculty of Electrical Engineering, University of Ljubljana. Currently, he is an Associate Professor at the same faculty. The research interests of Sašo Blažič include the adaptive, fuzzy and predictive control of dynamical systems and the modelling of nonlinear systems. Lately, the focus of his research is in the areas of autonomous mobile systems and satellite systems.

Drago Matko B.Sc., M.Sc. and Ph.D. in electrical engineering in 1971, 1973 and 1977 respectively, from the University of Ljubljana, Slovenia for work in the field of adaptive control systems. He visited the Institute of Space and Astronautical Science in Sagamihara Kanagawa, Japan as a Foreign Research Fellow for 9 months in 1995–1996 and for 6 months in 2003–2004. He received the award of Slovenian Ministry of Science and Technology for his work in the field of computer-aided design of control systems in 1989 and the Zois award for achievements in science in 2003.

Tomaž Rodič, B.Sc. and Ph.D. in mechanical engineering from the University of Ljubljana, Slovenia in 1986 and University of Wales, Swansea, UK in 1989, respectively. He was a postdoctoral fellow in DIMEG laboratories at the University of Padova in 1991–1992. In 1992 he established the Centre for Computational Continuum Mechanics in Ljubljana, Slovenia. He is a full professor at the Faculty of Natural Sciences and Engineering, University of Ljubljana and Director of SPACE-SI, the Slovenian Centre of Excellence for Space Sciences and Technologies.

Dejan Dovžan received B.Sc. degree in 2008 from the Faculty of Electrical Engineering, University of Ljubljana. In his bachelor thesis he covered self-tuning algorithms for the predictive functional controller and proposed solutions for better disturbance rejection of the PFC. He received a Prešeren award for this. He is currently employed at the Laboratory of Modeling, Simulation and Control at the Faculty of Electrical Engineering as a young researcher. His main research interests are in adaptive fuzzy control, predictive control, fuzzy modeling, fault detection using fuzzy models and recursive fuzzy identification, which is also the theme of his Ph.D. thesis.

Gašper Mušič received B.Sc., M.Sc., and Ph.D. in electrical engineering from the University of Ljubljana, Slovenia in 1992, 1995, and 1998, respectively. He is an Associate Professor at the Faculty of Electrical Engineering, University of Ljubljana. His research interests are in discrete event and hybrid dynamical systems, supervisory control, planning, scheduling, and industrial informatics.

Gregor Klančar received B.Sc. and Ph.D. degrees in electrical engineering from the University of Ljubljana, Slovenia in 1999 and 2003, respectively. He is currently employed as an Assistant Professor at the Faculty of Electrical Engineering at the University of Ljubljana. His research work focuses on the area of mobile robotics and on the area of control and supervision of multiagent systems.